Heterogeneity of strain and texture inside roll-bonded multilaminates

HANON Guillaume[1,a *], MALET Loïc[2,b] and DELANNAY Laurent[1,c]

[1]iMMC, UCLouvain, 1348 Louvain-la-Neuve, Belgium

[2]4MAT, Université Libre de Bruxelles, 1050 Bruxelles, Belgium

[a]guillaume.hanon@uclouvain.be, [b]loic.malet@ulb.be, [c]laurent.delannay@uclouvain.be

Keywords: Roll-bonding, anisotropic plasticity, Finite element

Abstract.
This study demonstrates the usefulness of crystal plasticity modeling and crystallographic texture analysis when aiming to understand through-thickness strain heterogeneity after roll bonding of dissimilar materials. FE modeling was used at two length scales to study the deformation and texture heterogeneities inside a 9-layer multilaminate made of aluminum and steel, produced by roll-bonding. Microstructure and crystallographic texture were probed using EBSD. Numerical predictions indicated that plane strain compression was accompanied by significant shear parallel to the rolling plane and inclined shear banding in aluminum. Predictions of the Texture development were more accurate in the bcc phase than the fcc phase.

Introduction

Roll bonding enables solid state welding of dissimilar metals in a single rolling pass, on the condition that thickness reduction is above 50% [1]. Due to the mismatch of strength, achieving co-deformation of the assembly is a challenge. The harder phase tends to fragment with the emergence of inclined shear bands inside the softer phase [2,3]. This undesirable result should be avoided or limited as it hinders achieving composite mechanical properties and is hence likely to reduce ductility, strength and toughness.

Previous investigations of the texture gradient across the thickness of rolled sheets have demonstrated that the plastic strain is heterogeneous even when the sheets are made of a single metal [4]. The amplitude of shear parallel to the rolling plane varies as a function of the depth across the sheet and also depending on the rolling draught, i.e. on the ratio between the thickness of the sheet and the contact length with the rolls [5,6]. To the knowledge of the authors, such studies have never been extended to the case of roll bonded composite multilayers.

The present study demonstrates that "macroscopic" Finite Element (FE) modeling of the through-thickness strain heterogeneity during rolling can efficiently be combined with "microscopic" crystal plasticity based finite element modeling (CPFEM) [7] of the texture development. The confrontation of numerical predictions and experimental observations is aimed to draw the link between deformation heterogeneity and through-thickness texture gradient.

Experimental samples

A 9-layer multilaminate was successfully roll-bonded at ambient temperature by stacking layers of 1050 aluminum alloy ($\sigma_{yield} = 75$MPa and $\sigma_{UTS} = 120$MPa) and Armco pure iron ($\sigma_{yield} = 250$MPa and $\sigma_{UTS} = 300$MPa). Before each rolling pass, all surfaces were degreased and brushed using a 0.3 mm diameter wire-brush, which removed oxide layers. Folding of the sheets impeded any relative motion between the layers [9]. The diameter of the rolls was 112 mm and no lubricant was used.

Two rolling passes were required to obtain the 9-layer stack. To start, a 3-layer was obtained by rolling a 0.8 mm-thick Iron sheet wrapped inside a 0.4 aluminum sheet folded in two. The first rolling pass involved 61% thickness reduction to ensure bonding. Two such 3-layers, stacked together with a central 0.2mm Fe layer, were then wrapped inside a 0.2 mm thick Fe sheet. The 9-layer multilaminate was heat treated (500°C for 30 minutes) before the second rolling pass of 62% thickness reduction.

Electron Back Scatter Diffraction (EBSD) was used to probe the crystallographic texture. A high level of surface finish was achieved by polishing up to grid 1200 with SiC paper, followed by diamond suspension up to 1 micron and OPS.

Figure 1 shows a section of the sample studied. Grey contrast in the optical microscope clearly identifies the 9 layers made of the two different metals. Four different zones were measured by EBSD, each one covering the plate thickness. One such orientation maps is shown in Figure 1 (blue square). Flat and elongated grains were found in all Fe layers whereas Al layers hosted a very refined equiaxed microstructure. Such microstructure is characteristic of continuous recrystallization [8,10]. The <111> pole figures shown in Fig. 1 are representative of individual layers. They were produced by combining suitable zones in the four orientation maps. Note that only the 7 central layers are represented as the indexing was poor (and the texture was weak) in the two peripheral layers.

Numerical simulations

Figure 2 gives an illustration of the two numerical models, working at different length scales, which assisted the interpretation of experimental pole figures. The commercial finite element code Abaqus/Standard (d'Assault Systèmes, France) was used for these two simulations.

The macroscopic strain field was predicted based on finite element modeling of the second rolling pass at the scale of the multi-layer. Only the half of the thickness was modelled as the strain field was symmetrical relative to the rolling plane (disregarding the emergence of instabilities). A total of 54576 2D Plane strain elements (CPE4) were used. Armco Iron and Pure Al alloys proprieties were assigned to the corresponding elements. Isotropic J_2 plasticity with a power-law hardening was prescribed as the material responses (reproducing the experimental yield stress and UTS). A friction coefficient of 0.3 was used [12]. The bonding was not simulated: layers were considered tied. Important shear deformation parallel to the rolling plane was predicted in the two aluminum layers as shown in Figure 2. The most external Al layer was subjected to the most intense shear deformation. This resulted from the large contact length (about 10 times the thickness of the sample) between the rolls and the plate, and also because the yield stress of Al layers was much lower than in Fe layers. Friction played a role too by inducing important shear deformation close to the external surfaces. Limited shear deformation was observed inside the Iron layers.

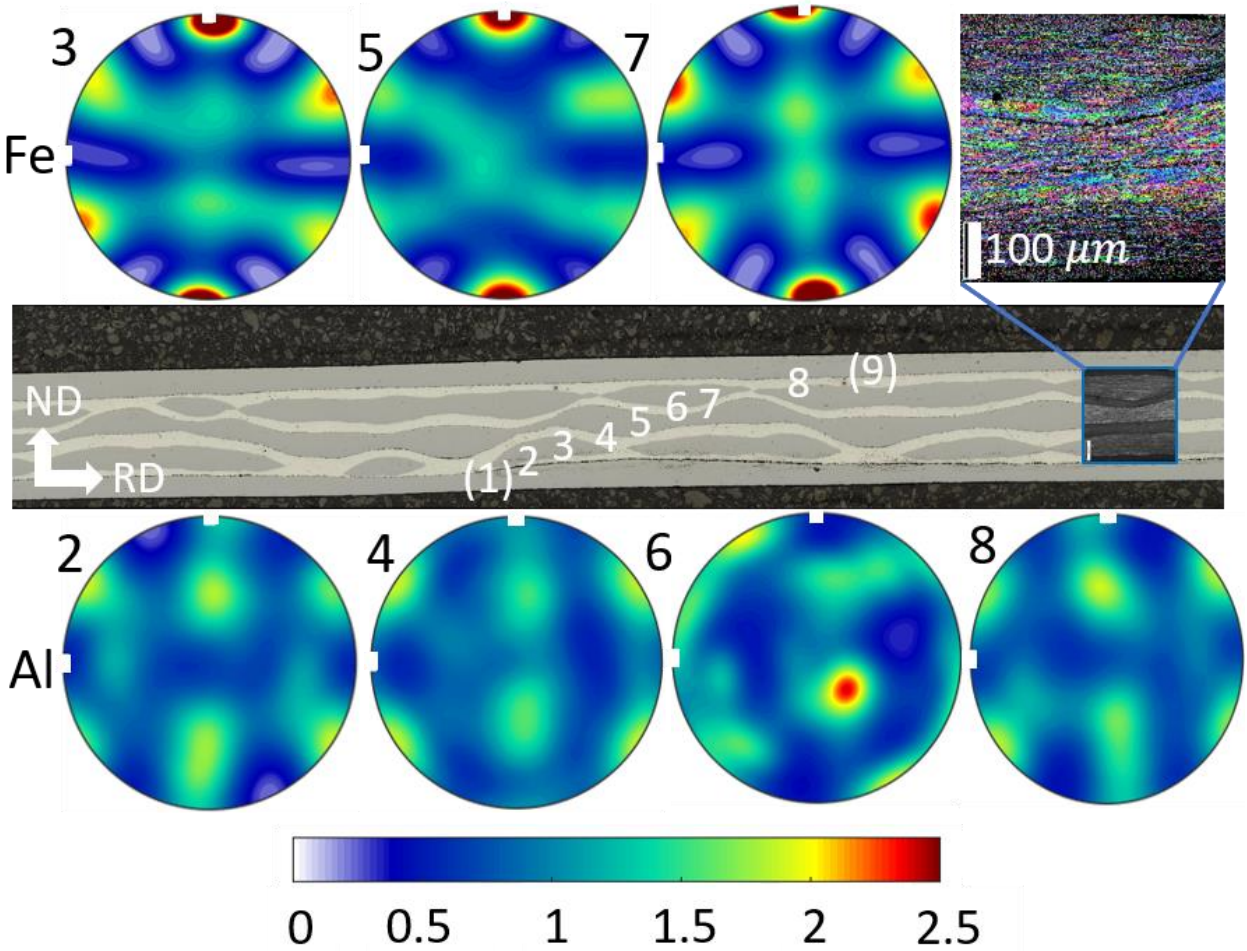

Figure 1: Characterization of texture and microstructure based on EBSD and optical microscopy. <111> Pole figures (numbered according to the position in the stacking) present the texture developed inside each layer in with the rolling direction (RD) pointing to the right and the normal direction (ND) pointing to the top.

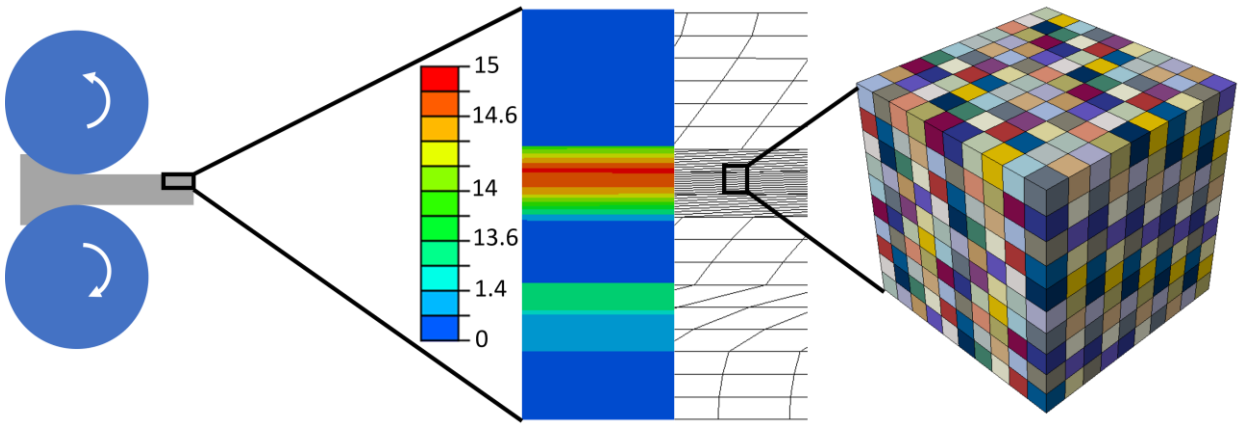

Figure 2: Illustration of the two scales of the FE analysis. On the left, the macroscopic through-thickness strain distribution was predicted during the 2nd rolling pass. The corresponding deformed

mesh is displayed alongside the RD-ND shear strain map. On the right, the model polycrystal was subjected to (microscopic) periodic boundary conditions.

Crystal Plasticity Finite Element Modeling (CPFEM) [7] allowed us to predict the texture development, respectively, inside Al and Fe layers. Anisotropic plasticity at the level of individual grains was implemented as a user-defined material law (UMAT). As usually assumed, the fcc phase was subjected to {111}<110> dislocation glide whereas the bcc phase allowed slip on both {110}<111> and {112}<111>. A simplified microstructure with brick-shaped grains was used. The domain was meshed with 9x9x9 elements (C3D20), each element corresponding to one grain. A random crystallographic orientation was initially assigned to each grain. Figure 2 shows this simplified microstructure where each colored element corresponds to a different grain. Periodic boundary conditions were applied so that peripheral grains behaved as if they were in the bulk of the polycrystal. Such CPFEM strategy was already validated in numerous previous studies [7].

The deformation inside the different layers was considered to be a combination of three different deformation modes: ND-RD plane strain compression, shear parallel to the rolling plane and shear banding tilted at 45° from the rolling direction. These different modes were first investigated individually to assess their impact on the evolution of texture. A deformation allowing to achieve 50% thickness reduction of the rolled sheet was prescribed in all cases.

As shown in Figure 3, shear parallel to the rolling plane induces anti-clockwise rotation ($\sim 15°$) of the pole figures that were predicted under orthotropic plane strain compression. Indeed, as highlighted in the figure, such shear is equivalent to compression along a direction that is inclined relative to RD. It is noteworthy that the (anticlockwise) rotation of the compression axis is opposite to the (clockwise) spin expected from shearing.

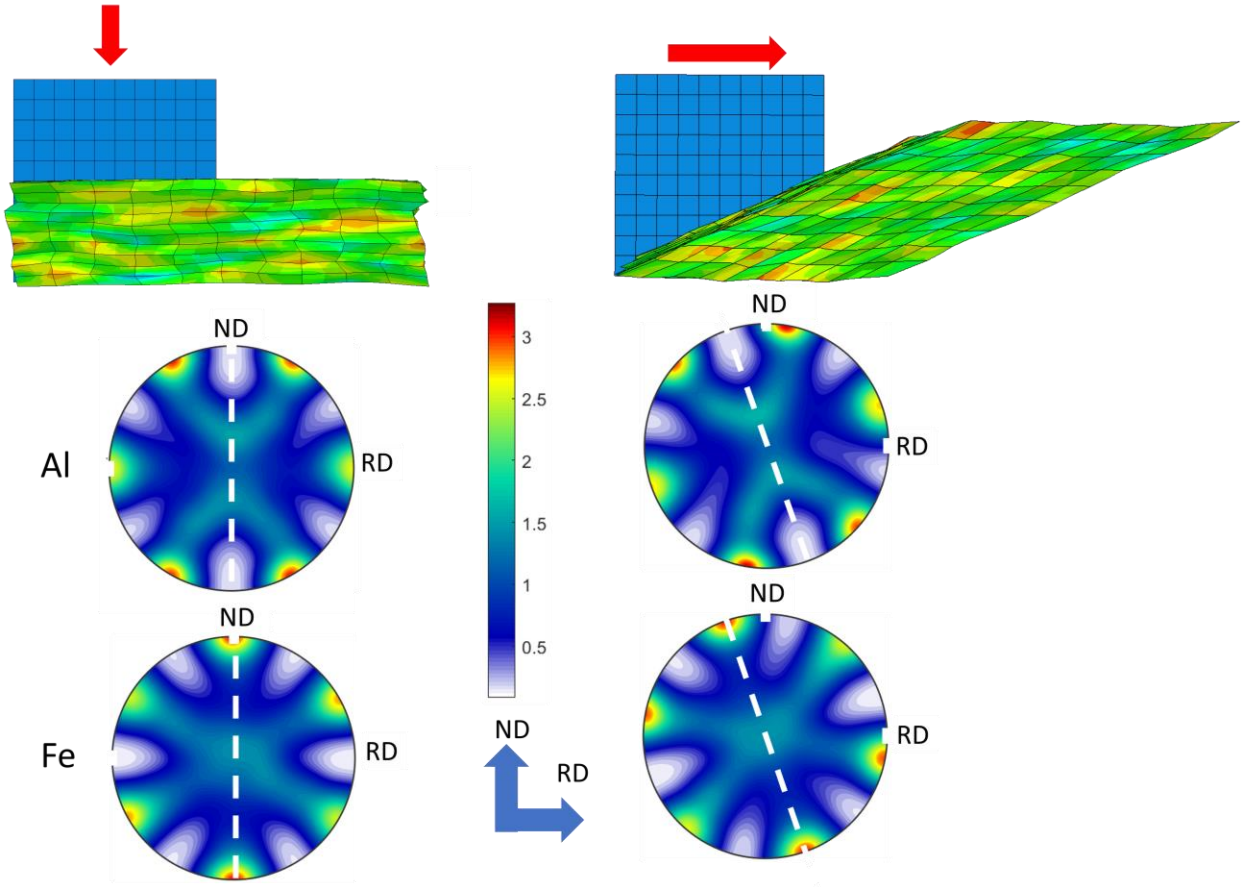

Figure 3: Compression and shear deformation modes. Textures predicted to develop inside Fe or Al are presented as <111> pole figures.

As shown in Fig. 4, the effect of shear bands inclined at +/-45° to the rolling direction is different. Such shear banding is equivalent to the superposition of orthotropic plane strain compression with rigid body rotation. The comparison of Fig. 3a and Fig. 4 shows that the pole figure rotation now conforms to the spin inside the shear band.

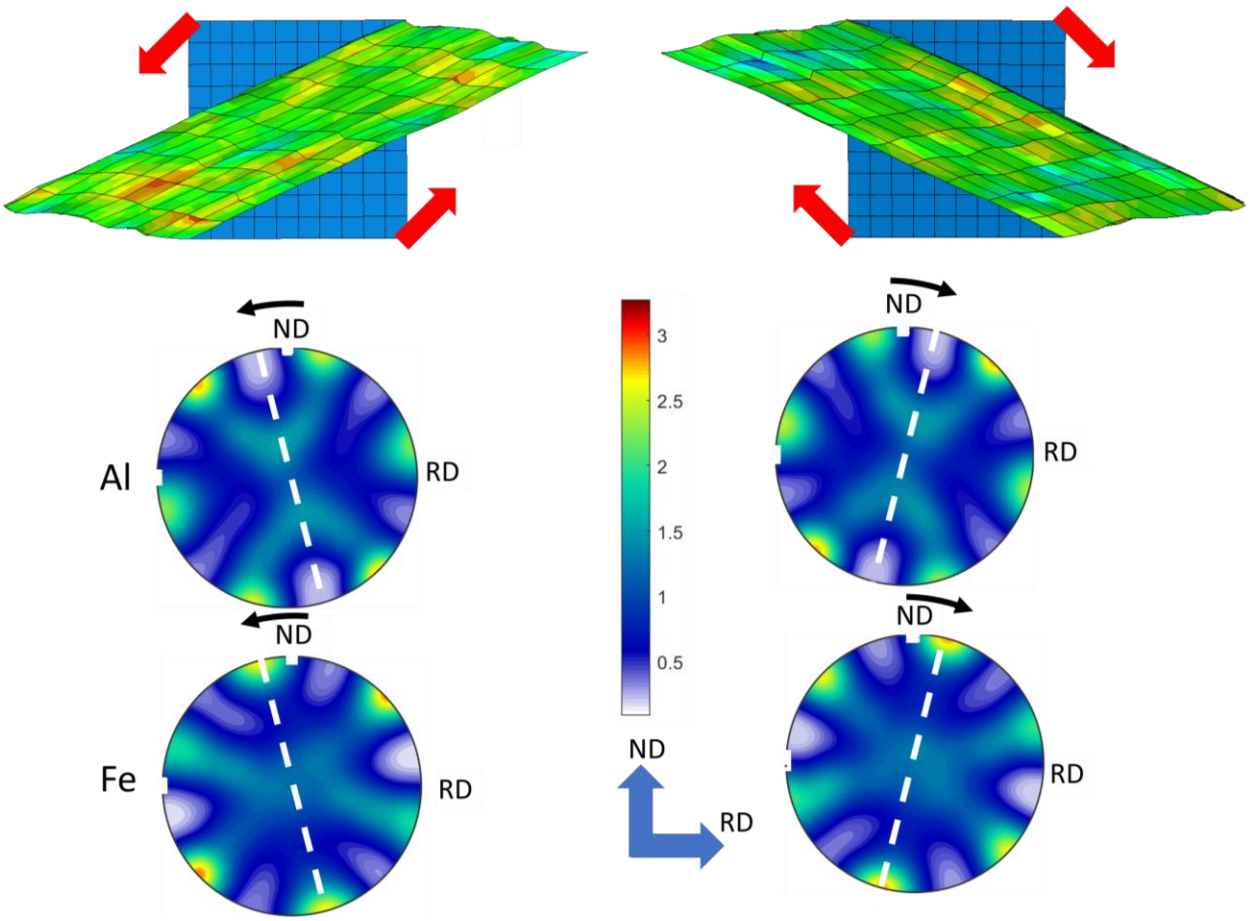

Figure 4: Positive shear band and negative shear band modes. Textures developed inside Fe or Al microstructures are presented as <111> pole figures.

The experimental pole figures shown in Fig.1 are representative of the mean texture in each layer so that the local effects of shear bands are suppressed. Figure 5 indicates, in a qualitative manner, the type of shear expected, respectively, in the upper and lower layers of the multilaminate.

Discussion

Textures in all the Fe layers, in Fig. 5, are close to conventional rolling textures predicted under plane strain compression. However, they are slightly rotated (~5°) in opposite directions on either side of the mid-thickness plane. This is consistent with the predictions of the macroscopic FE model: there is moderate shear parallel to the rolling plane in the hard phase. Note that the amplitude of rotation is much smaller than predicted in Figure 3 since there compression and shear occurred simultaneously in the real plate. The texture observed in the central Iron layer is orthorhombic indicating that shear was close to zero.

The EBSD measurements in aluminum reveal a weak “rotated cube” component. Such texture was already reported inside pure aluminum when continuous recrystallization occurred due to important shear deformation [8]. This too conforms to the prediction of the macroscopic FE model. Crystal plasticity predictions of the texture development were less accurate in Al including a {111}<112>, not observed experimentally. The prediction of rolling textures in fcc metals remains a challenge.

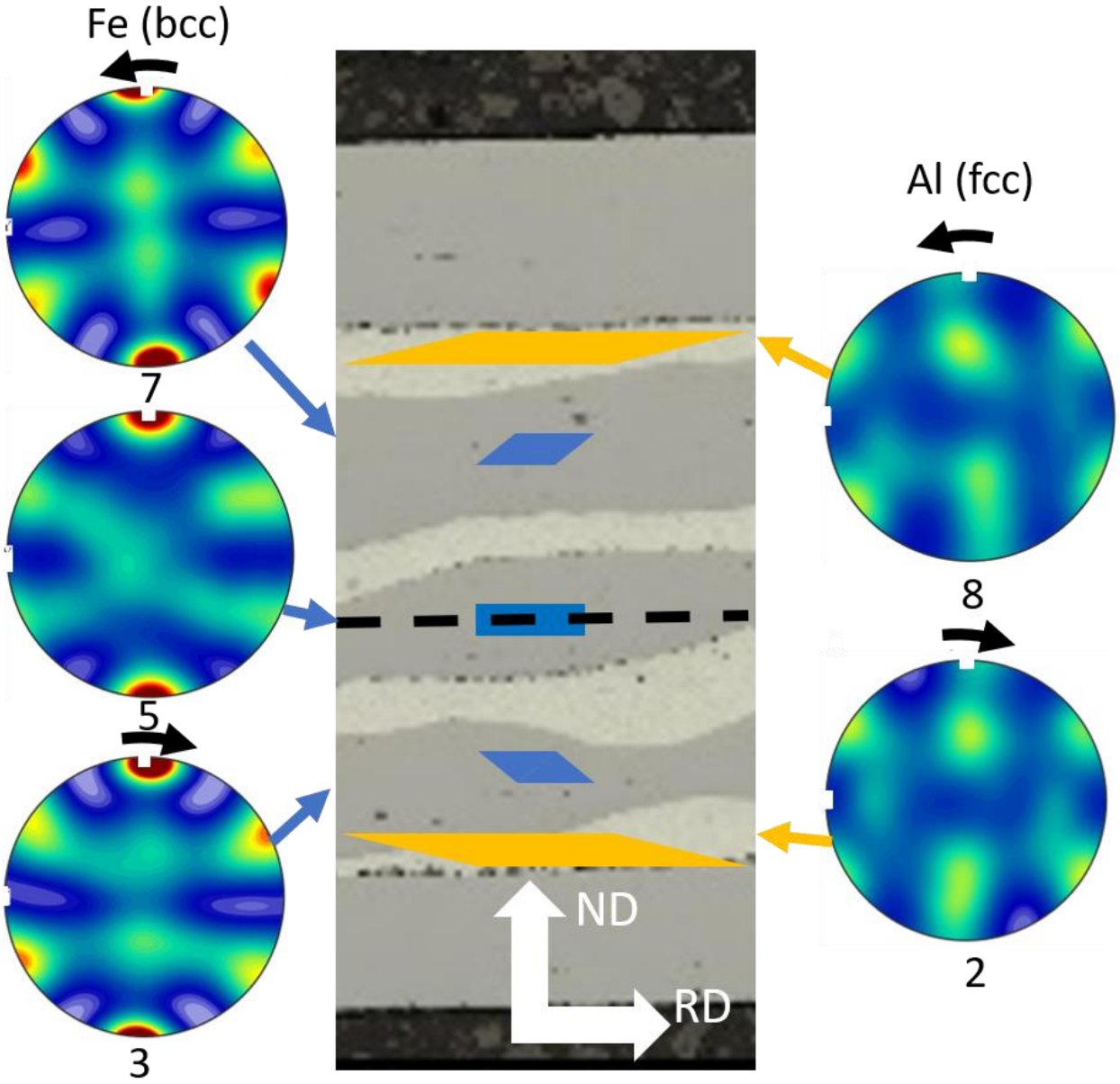

Figure 5: When considering shear parallel to the rolling plane, crystal plasticity predictions provide fair reproduction of the average texture inside each layer. The black arrows highlight the slight rotations relative to the orthorhombic texture expected under plane strain compression.

Conclusions

- After two rolling passes of a 9-layer multilaminate, the hard Fe layers was fragmented with the emergence of inclined shear bands inside the softer Al layers.

- According to macroscopic FE modeling of the through-thickness deformation gradient, significant shear occurred parallel to the rolling plane
- Crystal plasticity predictions confirmed that individual layers underwent significant shear parallel to the rolling plane. The influence of inclined shear bands was not seen when averaging the texture over a whole layer.
- The texture predictions were more accurate in steel than in aluminum layers. The latter layers hosted a rotated-cube component which is characteristic of continuous recrystallization under intense shear deformation.

Acknowledgements

Financial support for this work was provided by FNRS as well as by Eurofusion. LD is mandated by FNRS, Belgium. Computational resources were provided by the supercomputing facilities of the UCLouvain (CISM/UCLouvain) and the Consortium des Équipements de Calcul Intensif en Fédération Wallonie Bruxelles (CÉCI) funded by the Fond de la Recherche Scientifique de Belgique (F.R.S.-FNRS) under convention 2.5020.11 and by the Walloon Region.

References

[1] Hosseini, M., Pardis, N., Manesh, H. D., Abbasi, M., & Kim, D. I. (2017). Structural characteristics of Cu/Ti bimetal composite produced by accumulative roll-bonding (ARB). Materials & Design, 113, 128-136.

[2] McCabe, R. J., Nizolek, T. J., Li, N., Zhang, Y., Coughlin, D. R., Miller, C., & Carpenter, J. S. (2021). Evolution of microstructures and properties leading to layer instabilities during accumulative roll bonding of FeCu, FeAg, and FeAl. Materials & Design, 212, 110204.

[3] Govindaraj, N. V., Frydendahl, J. G., & Holmedal, B. (2013). Layer continuity in accumulative roll bonding of dissimilar material combinations. Materials & Design (1980-2015), 52, 905-915.

[4] Mishin, O. V., Bay, B., & Jensen, D. J. (2000). Through-thickness texture gradients in cold-rolled aluminum. Metallurgical and Materials Transactions A, 31, 1653-1662.

[5] Engler, O., Tomé, C. N., & Huh, M. Y. (2000). A study of through-thickness texture gradients in rolled sheets. Metallurgical and materials transactions A, 31(9), 2299-2315.

[6] Schoenfeld, S.E., Asaro, R.J.: Through thickness texture gradients in rolled polycrystalline alloys. Int. J. Mech. Sci. 38(6), 661–683 (1996)

[7] Lin, F., Marteleur, M., Jacques, P. J., & Delannay, L. (2018). Transmission of {332}< 113> twins across grain boundaries in a metastable β-titanium alloy. International Journal of Plasticity, 105, 195-210.

[8] Li, Z., Li, L. Y., Zhu, Y. B., Lin, K., Ren, Z. T., Yang, Y., ... & Langdon, T. G. (2022). Evidence for a stable single component sharp texture in high purity aluminum during tube high-pressure shearing at room temperature. Scientific Reports, 12(1), 17901.

[9] Hanon, G., Malet, L., Delannay, L. (2023). Texture and Microstructure After Roll-Bonding of an Fe-Al Multilaminate. In: Mocellin, K., Bouchard, PO., Bigot, R., Balan, T. (eds) Proceedings of the 14th International Conference on the Technology of Plasticity - Current Trends in the Technology of Plasticity. ICTP 2023. Lecture Notes in Mechanical Engineering. Springer, Cham.

[10] Sidor, J., Petrov, R., & Kestens, L. (2014). Texture control in aluminum sheets by conventional and asymmetric rolling. In Comprehensive materials processing, vol. 3: advanced forming technologies (pp. 447-498). Elsevier.

[12] Tieu, A. K., & Liu, Y. J. (2004). Friction variation in the cold-rolling process. *Tribology International*, *37*(2), 177-183.